

The stellar wind of the Crab supernova's progenitor

Paul Murdin^{1,2}★

¹Royal Observatory, Blackford Hill, Edinburgh EH9 3HJ

²Royal Greenwich Observatory, Madingley Road, Cambridge CB3 0EZ

Accepted 1994 February 7. Received 1994 February 3; in original form 1993 December 8

ABSTRACT

Between 4 and 9 solar masses of the progenitor of the Crab nebula supernova are missing, unaccounted for in the filaments and pulsar. Deep spectroscopy and a re-analysis of a direct Schmidt telescope image show a hydrogen-emitting halo around the Crab nebula which can be satisfactorily interpreted as the low-velocity stellar wind of the progenitor. The halo's mass is about 4 solar masses; the progenitor of SN 1054 was thus about 8 solar masses.

Key words: stars: mass-loss – supernovae: individual: SN 1054 – ISM: individual: Crab nebula – supernova remnants.

1 INTRODUCTION

The Crab nebula is the remnant of the supernova of 1054; its recognized massy parts are a pulsar, and expanding filaments. The mass of the pulsar is about 1.4 times that of the Sun. The mass of the filaments can be estimated by fitting theoretical line-strength calculations to spectrophotometry. The consensus is that the mass of the filaments is probably 1–2 M_{\odot} (O'Dell 1962; Henry & MacAlpine 1982; Davidson & Fesen 1985; MacAlpine et al. 1989; MacAlpine & Uomoto 1991), although some estimates range up to 6 M_{\odot} .

The pulsar is interpreted as the neutron star formed in the collapse of the core of the progenitor star, and the filaments as the exploding body of the star. This is the description of a Type II supernova (and the Type Ib,c subtypes). Indeed, SN 1054 had a light curve which, although not well determined, may have been more typical of Type II than Type Ia (Minkowski, quoted by Murdin & Murdin 1984). If the contemporary observations leave the classification of SN 1054 in doubt, there is no doubt that the filaments now have strong hydrogen emission, although the filamentary ejecta have not swept up large amounts of interstellar hydrogen (since the nebula is small and the density of interstellar material at the relatively high-galactic-latitude position of the Crab is low). The implication is that hydrogen emission would have been detected in the spectrum of SN 1054, had there been spectrographs to observe it at the time, and this is consistent with Type II.

If SN 1054 was of Type II, its progenitor star had a mass initially of at least 8 M_{\odot} , else it would not have exploded (van den Bergh 1994). The filaments show abundances of the elements (helium is overabundant compared to the Sun, but oxygen is normal) which together imply that the initial mass of the progenitor was less than 13 M_{\odot} (Nomoto 1985). Thus a mass for the Crab nebula of between 8 and 13 M_{\odot} is required, but only about 4 M_{\odot} is seen in the pulsar and filaments; a significant amount of the progenitor star is unaccounted for.

Chevalier (1977, 1985, 1994) has suggested that this material lies in a faint halo, either a fast envelope (Lundqvist, Fransson & Chevalier 1986), or a pre-supernova stellar wind. Observational evidence for the fast envelope has been at best ambiguous. Clark et al. (1983) and Deneffeld & Pequignot (1983) detected line emission in the central area of the Crab, interpreted as high-velocity material in the range 2400 to 3600 and even 5200 km s^{-1} , but Fesen & Ketelsen (1985) could not confirm high-velocity material to a limit of $3 \times 10^{-15} \text{ erg s}^{-1} \text{ cm}^{-2}$ from a central area of $14 \times 35 \text{ arcsec}^2$. Certainly, deep imaging does not show detectable *knots* outside the boundary of the Crab. There is doubt, therefore, that the Crab halo is high-velocity material.

However, Murdin & Clark (1981) detected, by deep wide-angle UK Schmidt Telescope photography through a 150-Å H α filter, a faint *diffuse* halo surrounding the Crab, extending up to 14 arcmin from the pulsar. The halo has a surface brightness of order $2 \times 10^{-7} \text{ erg s}^{-1} \text{ cm}^{-2} \text{ sr}^{-1}$, corresponding to an emission measure of $7 \text{ cm}^{-6} \text{ pc}$.

This detection of the halo has not, until now, been confirmed. Davidson & Fesen (1985) reported that deep images made with an intensified Image Tube Camera on a 0.9-m telescope in narrow-passband [O III] and H α + [N II] by Gull

★ Present address: Particle Physics & Astronomy Research Council, Polaris House, Swindon SN2 2SZ.

& Fesen (1982) did not show the halo, but neither the point-spread-function of the detector nor quantitative upper limits were given. Radio searches (Wilson & Weiler 1982; Matveenko 1984; Velusamy 1984) for supernova-remnant-like synchrotron emission from the halo have all been negative.

The present paper presents the result of a new treatment of the deep photograph showing the halo, and confirms its existence by spectroscopy. The halo is interpreted as the progenitor's stellar wind.

2 OBSERVATIONAL DATA

The imaging data are from the same deep UK Schmidt Telescope H α plate used by Murdin & Clark (1981). [Since the following incident has been incompletely reported (Davidson 1985), I note that this plate was lost during my transfer from Australia to the UK and has been missing for over 10 years; it was rediscovered in 1993 in the RGO plate library, following the relocation of the RGO from Herstmonceux to Cambridge.] The central 55 arcmin of the plate has been scanned by the COSMOS facility of the UK Wide Field Astronomy group at the Royal Observatory Edinburgh, with a pixel size of 16 μm (1 arcsec) rebinned by a factor of 6.

The spectroscopic data are from the La Palma data archive, and were obtained with the 2.5-m Isaac Newton Telescope and Intermediate Dispersion Spectrograph with the Image Photon Counting System as a detector (set to have a pixel size 0.5 $\text{\AA} \times 2.8$ arcsec). The principal data sum to a deep exposure (nearly 7 h) of the H β and [O III] spectrum in a section east–west across the boundary of the Crab nebula, centred on the star (hereafter called star A) near RA 05^h31^m21^s.6, Dec. +22°00'25" (1950), and passing near the fainter star (hereafter star B) lying 20 arcsec west [see Woltjer 1957, where, in his fig. 2, star A is at coordinates (+12.5, +8) and star B at (+14, +8)]. The region of the spectrum extended 3 arcmin west of the star into the north-western quadrant of the Crab's halo, as well as 3 arcmin east across the central region of the nebula. A second set of shorter exposure data taken across the jet to the north of the Crab nebula was also available from the same archive collection.

3 OBSERVATIONAL RESULTS

The direct image produced by COSMOS (Fig. 1a) shows, in the raw data, portions of a halo around the Crab nebula. The image has been median-filtered (Fig. 1b) on a scale of 15 pixel, i.e. 90 arcsec, to remove most of the structure due to stars. About 20 bright stars still show as point sources; apart from these, the filtered image also shows an enhanced faint-star background to the north and east. The faint halo has become more readily visible in the filtered data.

The point-spread-function of the original plate material (see Murdin & Clark 1981) showed from the outset that this halo is *not* an instrumental effect (Davidson & Fesen 1985); it is too bright and widely extended to be scattered light from the Crab. This is confirmed by its spectrum, which is completely different from the spectrum of the Crab nebula (see below). It is interesting that the shape of the halo has some similarities with the shape of the outermost isophote of the Crab nebula shown by Woltjer (1957). The shape of the halo seems to follow the elliptical outline of the Crab nebula; Chevalier (1985) pointed out that this is surprising.

East of star B, which marks the north-western boundary of the Crab nebula supernova remnant, the La Palma spectra show, at all slit positions, synchrotron continuum and high-velocity material. The spectra at slit positions west of star B, in the halo of the Crab nebula, show, by contrast, a low-velocity H β spectral line (Fig. 2) from a diffuse emission nebula. In the same region where low-velocity H β is present, west of star B, there is no corresponding spectral emission from [O III]; [O III]/H β < 0.2, in contrast to the Crab filaments where [O III] is several times stronger than H β . Although Davidson & Fesen (1985) report no detection of the halo by Gull & Fesen (1982), it is interesting to note that their H α image shows a more diffuse appearance than the corresponding [O III] image, which shows an exceptionally sharp, cleanly delineated boundary to the Crab at this edge.

The H β spectral line in Fig. 2 is not resolved by the instrument; its full width at 1/e corresponds to 60 km s⁻¹. Its mean radial velocity of +38 \pm 28 km s⁻¹ is indistinguishable from zero, and consistent with virtually everything in the Galaxy at the Crab's anticentre galactic longitude. A higher resolution spectrum would obviously be of interest in resolving the wind velocity, determining the Galactic radial velocity of the Crab nebula, showing if the progenitor was a runaway star (at the relatively high galactic latitude), etc.

The H β emission extends (Fig. 3) from the outermost edge of the Crab nebula to the end of the spectrograph slit, i.e. to 3 arcmin west of star A, up to 4 arcmin from the pulsar. The intensity of the spectral line generally increases towards the Crab, reaching a maximum at star B. Just interior to star B, its intensity decreases abruptly, and further into the nebula it becomes undetectable amongst the high-velocity ejecta (Fig. 4).

The spectral profile of the narrow H β line is completely different from the profile of the brighter filamentary emission; moreover, there is no similar phenomenon for [O III]. This shows that the narrow line is not any scattered-light phenomenon from the Crab. The spatial variation of the H β emission on an angular scale as small as 2 arcsec (Fig. 4) shows that it is certainly not an atmospheric phenomenon.

Could the halo be Galactic diffuse emission? Galactic diffuse emission is seen in Balmer lines, and faintly in [O III] among other spectral lines. It has been modelled by Mathis (1986) as low-density gas photoionized by distant O-type stars. Reynolds (1987) shows the latitude variation of H α intensity outside the most prominent H II region enhancements at a longitude of 213°; at the latitude of the Crab, $b = +6^\circ$, the H α intensity is 7.5 \pm 3 Rayleigh, typically with 150 km s⁻¹ width. The intensity of the H β line detected in the Crab halo is on the whole higher, and its linewidth is different.

Galactic diffuse emission varies on a scale of degrees, whereas the halo varies on a scale of seconds of arc – the narrow H β emission decreases abruptly by over a factor of 2 (about 1 mag) at the outermost edge of the high-velocity ejecta, as is evident in Figs 3 and 4. Could this be due to extinction of background emission by material in the Crab? From star counts, the overall extinction due to the Crab is less than 0.2 mag (Trimble 1977). Dust in the Crab has been detected by its visible extinction in isolated regions (0.8 to 5 arcsec in diameter) with extinction values up to 0.44 mag, and by a thermal infrared excess, interpreted as warm dust and perhaps correlated with an overall dust extinction of less

than 0.08 mag (Fesen & Blair 1990). Thus the large decrease in $H\beta$ emission cannot be due to absorption of background light by the sparse dust material in the Crab.

On the grounds, therefore, of intensity, linewidth, spatial variation and spatial coincidence, it seems unlikely that the halo is Galactic diffuse emission. The variation of $H\beta$ emission is a strong indication that the $H\beta$ emission arises in a halo abutting the Crab nebula. The natural interpretation is that the halo material is centred on the Crab, and is being run into by the ejecta at the edge of the Crab nebula.

Analysis of the second set of spectra from the same archive, taken across the Crab nebula jet, confirms the

presence of low-velocity $H\beta$ emission extending 2 arcmin north of the northern edge of the main body of filaments either side of the jet structure, with a similar anticorrelation with filamentary emission; it has not proved possible to map the $H\beta$ emission, however, because the second set of spectra (which, unlike the spectra of Figs 2–4, were taken at different times) cannot be confidently calibrated to a common internal photometric standard.

The principal set of $H\beta$ spectra have been calibrated to surface brightness units by reference to a spectrophotometric standard star (EG 248) observed during the observing run and using the geometry of the spectrograph slit (3.1 square

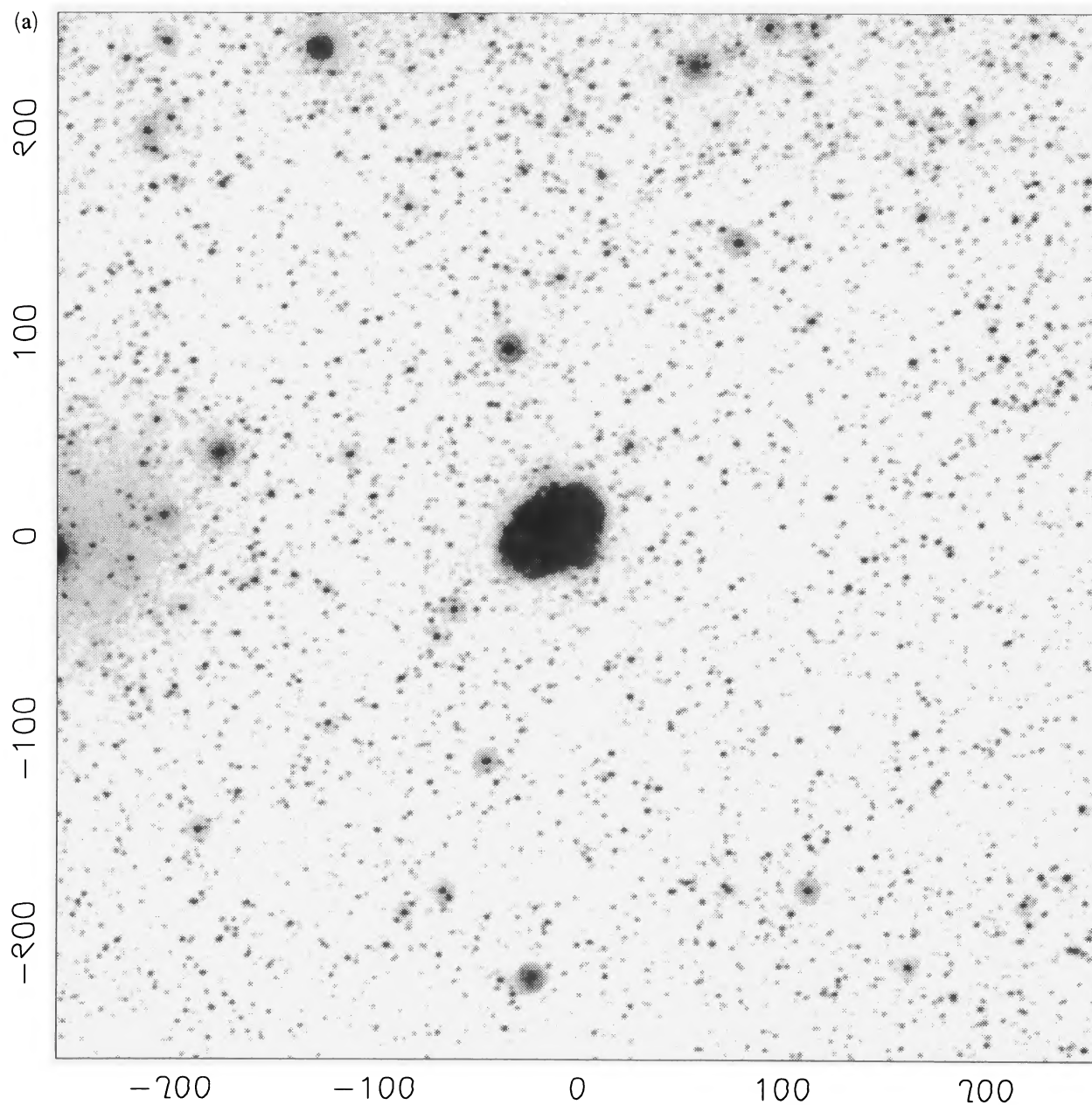


Figure 1. (a) The Crab nebula and field stars. The UK Schmidt Telescope $H\alpha$ image, scanned by COSMOS at ROE, is 55 arcmin square, binned to a 6-arcsec resolution (the units of the coordinate system of the map), and shows the Crab nebula at the centre, with traces of the halo visible out to 2 arcmin from the edge of the nebula.

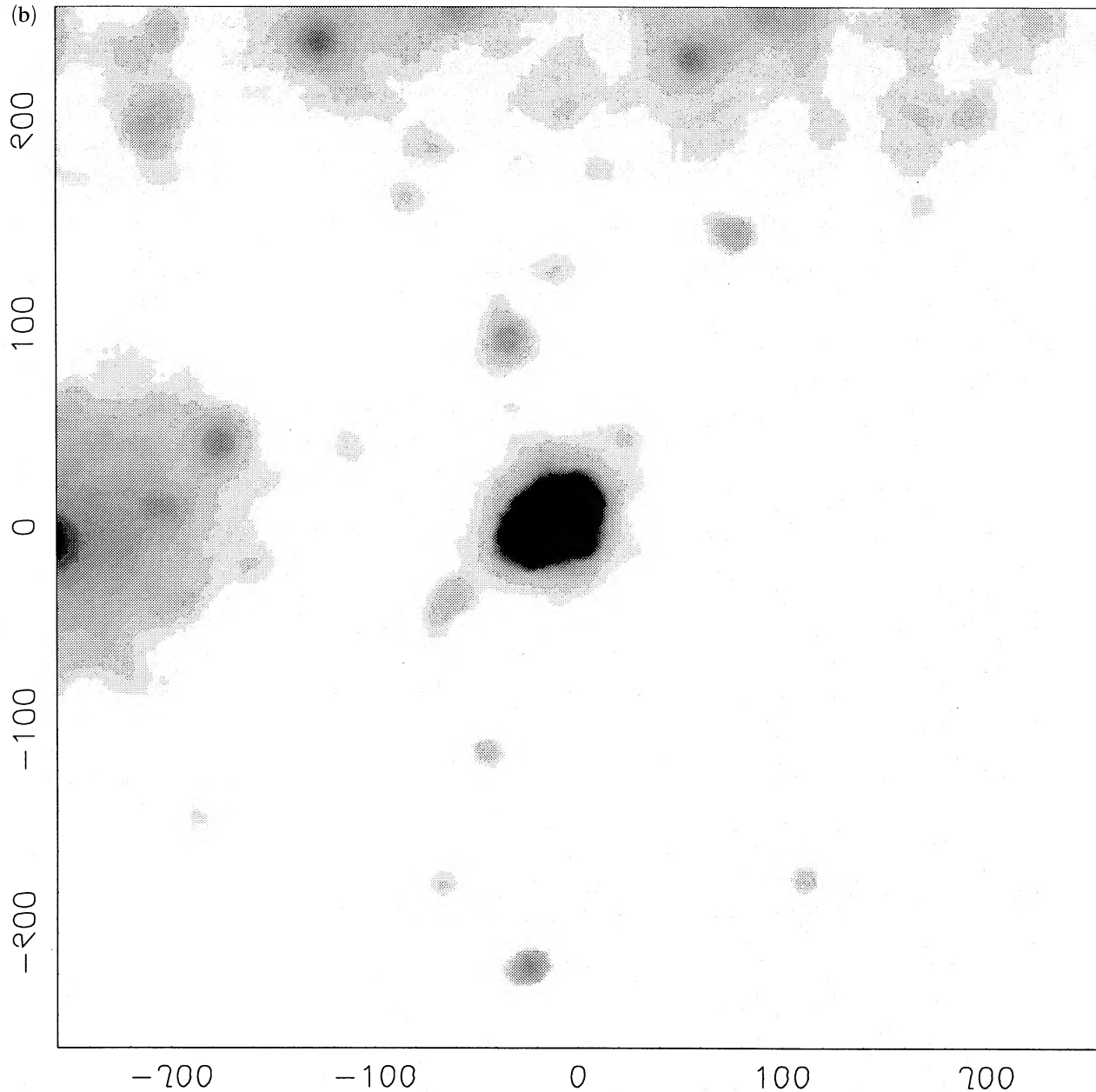


Figure 1. (b) The Crab nebula. After median-filtering on a 90-arcsec scale, all field stars except the 20 or so brightest ones are removed; the halo can be seen extending to about 6-7 arcmin from the pulsar.

arcsec pixels). The calibration differed by only 4 per cent from a calibration made by referring the continuum radiation through the spectrograph slit to a profile of the synchrotron emission presented as isophotes by Woltjer (1957).

The surface brightness flux was transformed to emission measure by the following procedure. The $H\beta$ flux from the halo is related to the $H\alpha$ flux by the case B Balmer decrement (Osterbrock 1989), $H\alpha/H\beta = 2.93$. This has to be corrected for reddening using $A_V = 1.6$ mag for the Crab nebula (Miller 1973). Reynolds (1987) gives the relationship between $H\alpha$ surface brightness, $I(\alpha)$ measured in Rayleigh, and emission measure, EM , as

$$\begin{aligned} 1 \text{ Rayleigh} &= 10^6/4\pi \text{ photon cm}^{-2} \text{ s}^{-1} \text{ sr}^{-1} \text{ cm}^{-2} \\ &= 2.4 \times 10^{-7} \text{ erg cm}^{-2} \text{ s}^{-1} \text{ sr}^{-1} \text{ at } H\alpha \end{aligned}$$

and

$$EM = 2.75 (T/10\,000)^{0.9} I(\alpha) \exp[2.2 E(B-V)] \text{ cm}^{-6} \text{ pc.}$$

In this formula, I set $T = 7000$ K. This is the same value as for the Galactic diffuse emission (Reynolds 1987), a value that is typical for an $H\text{ II}$ region. This is, however, an assumption. It may underestimate the temperature of the halo if it is heated by energetic particles and synchrotron emission from the Crab nebula, as proposed by Lundqvist et al. (1986). Alternatively, it may overestimate the temperature if the halo was ionized by the supernova outburst in 1054 and has since cooled.

With this estimate of temperature, I can form (Fig. 5) a profile showing the EM of the Crab halo as a function of distance R arcmin from the pulsar. The profile of Fig. 5 also

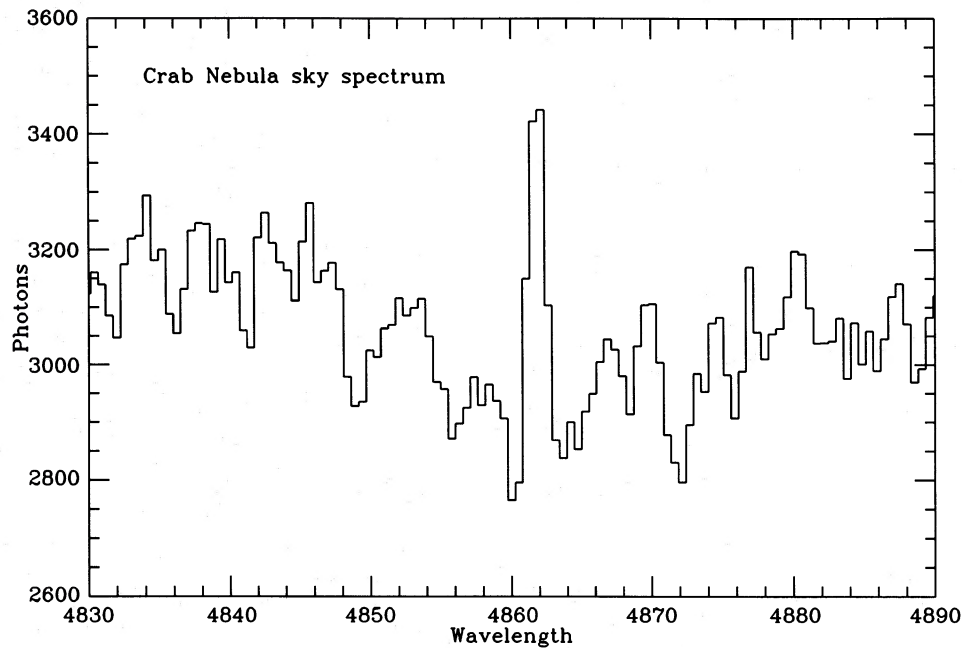


Figure 2. Spectrum of the sky near the Crab nebula. The spectrum shows a narrow emission line at $H\beta$ superimposed on a continuum from background starlight, etc., and centred on a broad absorption line of $H\beta$ from the zodiacal light. This spectrum shows the detected photons in 6.5 h from the sum of increments 6–37 (area 99 arcsec²), which are shown spatially resolved in Fig. 3.

shows the EM of the halo detected by Murdin & Clark (1981). The spectroscopic and photometric measurements are consistent, even though the spectroscopic cut and the four photometric cuts are in three different directions in the halo, and the calibration of the photometry was approximate.

4 INTERPRETATION

The halo might perhaps be an $H\text{II}$ region centred on the Crab and formed from dispersed material in the interstellar medium. Cas A is a Type II supernova remnant which shows such a surrounding $H\text{II}$ region (van den Bergh 1971), which is bright, extended and massive (dereddened emission measure is some $1 \times 10^4 \text{ cm}^{-6} \text{ pc}$, radius 5.7 pc, mass $6 \times 10^2 M_{\odot}$). The halo around the Crab is much fainter, more compact and much less massive (see below); moreover, the Crab nebula's high galactic latitude is an additional reason why the halo is not an $H\text{II}$ region.

The more likely origin of the halo appears to be a low-velocity stellar wind ejected during the red supergiant stage of the Crab nebula progenitor's evolution, as proposed by Chevalier (1977, 1985, 1994). The analogy with the circumstellar material visible around SN 1987A in the LMC is clear, except that the wind material from SN 1987A's progenitor was certainly ionized only by the supernova UV flash (as may be the $H\text{II}$ region associated with Cas A).

The emission measure should form an inverse cube relationship with radius, if the halo has been formed from an extensive, spherically symmetric, outflowing, steady wind of constant speed. (The asymmetric distribution of the circumstellar material of SN 1987A and the elliptical shape of the Crab nebula indicate that this assumption is highly idealized.) Fig. 5 shows such a relationship, which, in the circumstances,

is a satisfactory fit to the data between $R = 2.8$ arcmin and about 8 arcmin. To the extent that the data are fitted by the inverse-cube law, this is consistent with the stellar-wind model.

The distance of the Crab nebula is in the range 1030 to 2170 pc, with the most probable value lying near the middle of the range (Trimble 1970, 1973), say 1500 pc. The equation of the straight line in Fig. 5 is thus

$$EM = AR^{-3},$$

where $A = 4.9 \times 10^{75}$ cgs units: (atom of hydrogen $\text{cm}^{-3})^2 \text{ cm}^4$.

For a wind of constant velocity v and constant mass-loss rate of dm/dt ,

$$A = (dm/dt)^2 / 32\pi v^2.$$

Thus $(dm/dt)/v = 7.0 \times 10^{38}$ atom of hydrogen $\text{s}^{-1} (\text{cm s}^{-1})^{-1}$.

The mass-loss rate dm/dt is thus $1.8 \times 10^{-5} M_{\odot} \text{ yr}^{-1}$ if $v = 10 \text{ km s}^{-1}$. Radio emission from Type II supernovae indicates mass-loss rates of $1-2 \times 10^{-4} M_{\odot} \text{ yr}^{-1}$, and, from related Type Ib,c supernovae, rates of $1-2 \times 10^{-6} M_{\odot} \text{ yr}^{-1}$ (Van Dyk et al. 1993); the mass-loss rate of the Crab's progenitor appears to have been between the two values. If $v = 10 \text{ km s}^{-1}$ and the halo extends from 2.8 arcmin (1.2 pc = $3.7 \times 10^{13} \text{ km}$) to 8 arcmin (3.6 pc = $11 \times 10^{13} \text{ km}$), the halo was formed in 220 000 yr, and the total mass loss in this period was $3.9 M_{\odot}$.

This estimate of the mass lost to the halo is independent of the assumed value of v , and scales as $1/\sqrt{d}$, where d is the assumed distance of the Crab. The estimate does, of course, depend on the accuracy of the fit in Fig. 5 and the ideal

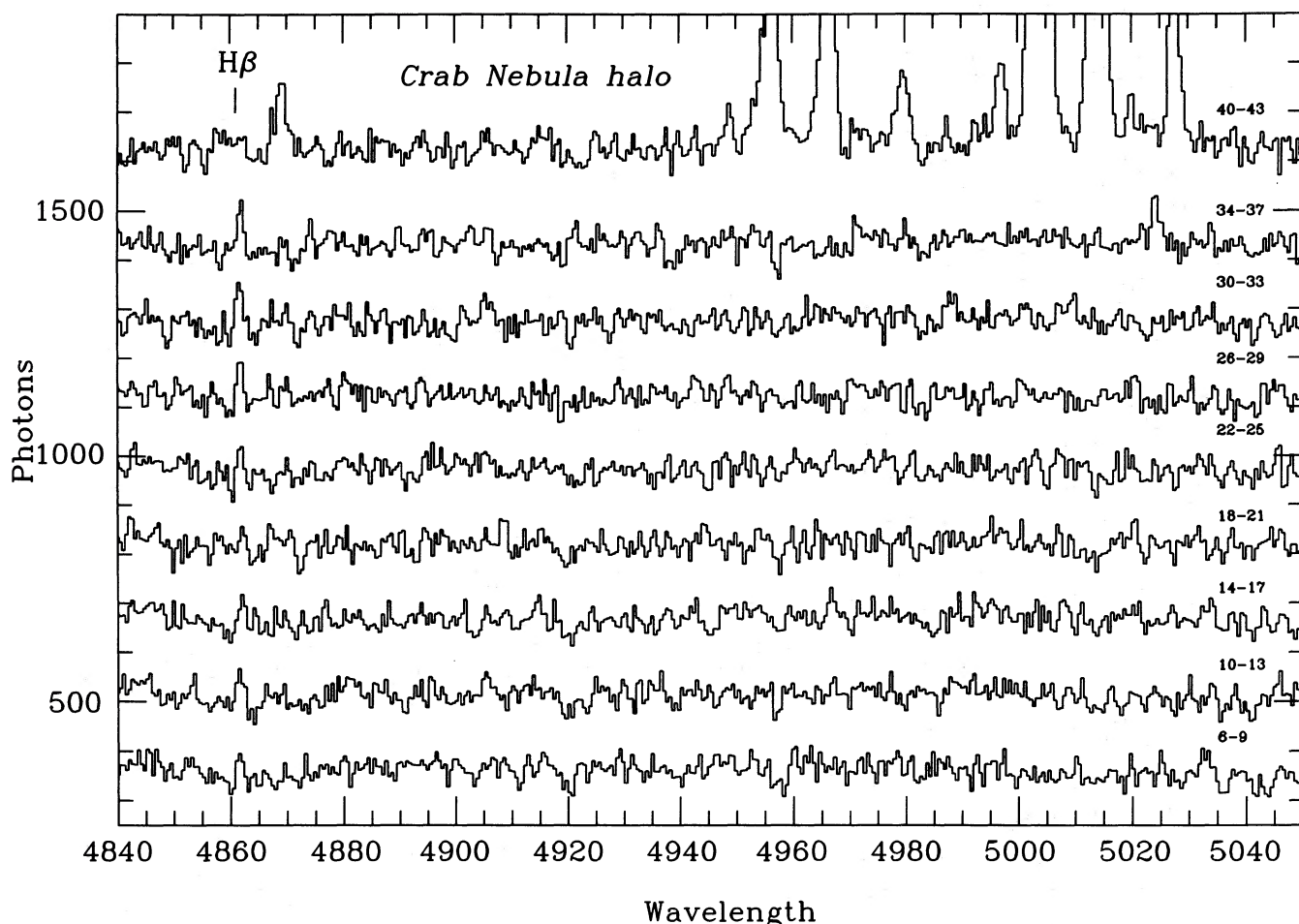


Figure 3. Spatially resolved spectra of the sky near the Crab nebula. Each spectrum shows the photons detected from a 6.5-h integration of four adjacent areas of sky, each 2.8 arcsec long and 1.1 arcsec wide. The y-scale of detected photons is correctly zeroed only for the bottom spectrum; other spectra are offset by arbitrary amounts in y. The right-hand numbers label the spectra in incremental areas along the slit, increasing towards the east, into the nebula. Star B fills increments 38 and 39, and these two areas are omitted from the plot. High-velocity, [O III]-emitting filaments are numerous and plain in increments 40–43 plotted at the top of this figure; although high-velocity H β emission is weaker, the H β absorption line of the zodiacal light is infilled by broad emission in the top spectrum, and a high-velocity knot of H β shows at 4868 Å. High-velocity [O III] can be detected as starting in increment 37 (a high-velocity knot due to [O III] 5007 shows at 5025 Å in the spectrum labelled 34–37). H β can be clearly detected at near-zero velocity shift in all spectra between increments 6 and 37, except perhaps increments 18–21. The H β emission generally increases in strength towards the Crab nebula, and abruptly decreases at star B in increment 38. There is no corresponding [O III] emission.

assumption about the geometry of the mass loss, i.e. constancy and spherical symmetry. Figs 3 and 4 appear to show, too, that the halo is clumpy.

On the assumption of constant mass outflow, the mass of the stellar wind interior to the position that the filaments have now reached was some $[2.8/(8-2.8)] \times 3.9 M_{\odot}$, i.e. $2 M_{\odot}$; this will be an upper limit if, after its red supergiant stage, the Crab progenitor passed through a blue supergiant stage with a fast, low-density wind which swept a central hollow.

Fig. 5 shows a preliminary model in which the stellar wind has such a hollow, and is bounded by two spheres, an

inner one at 2.8-arcmin radius and an outer one at 8 arcmin. In such a spherically symmetric, hollow model, the emission measure would remain approximately constant across the face of the Crab nebula, but it has proved impossible to detect in the data faint zero-velocity H β emission among the bright emission from the central filaments. There is some difficulty for this model to accommodate the sharpness and amplitude of the change in emission measure at the inner boundary at the edge of the ejecta (see the inner region of the data in Fig. 5). This may indicate that the halo is not spherically symmetric (as the circumstellar ring around SN 1987A). In any case, the scatter of the data is large (as a

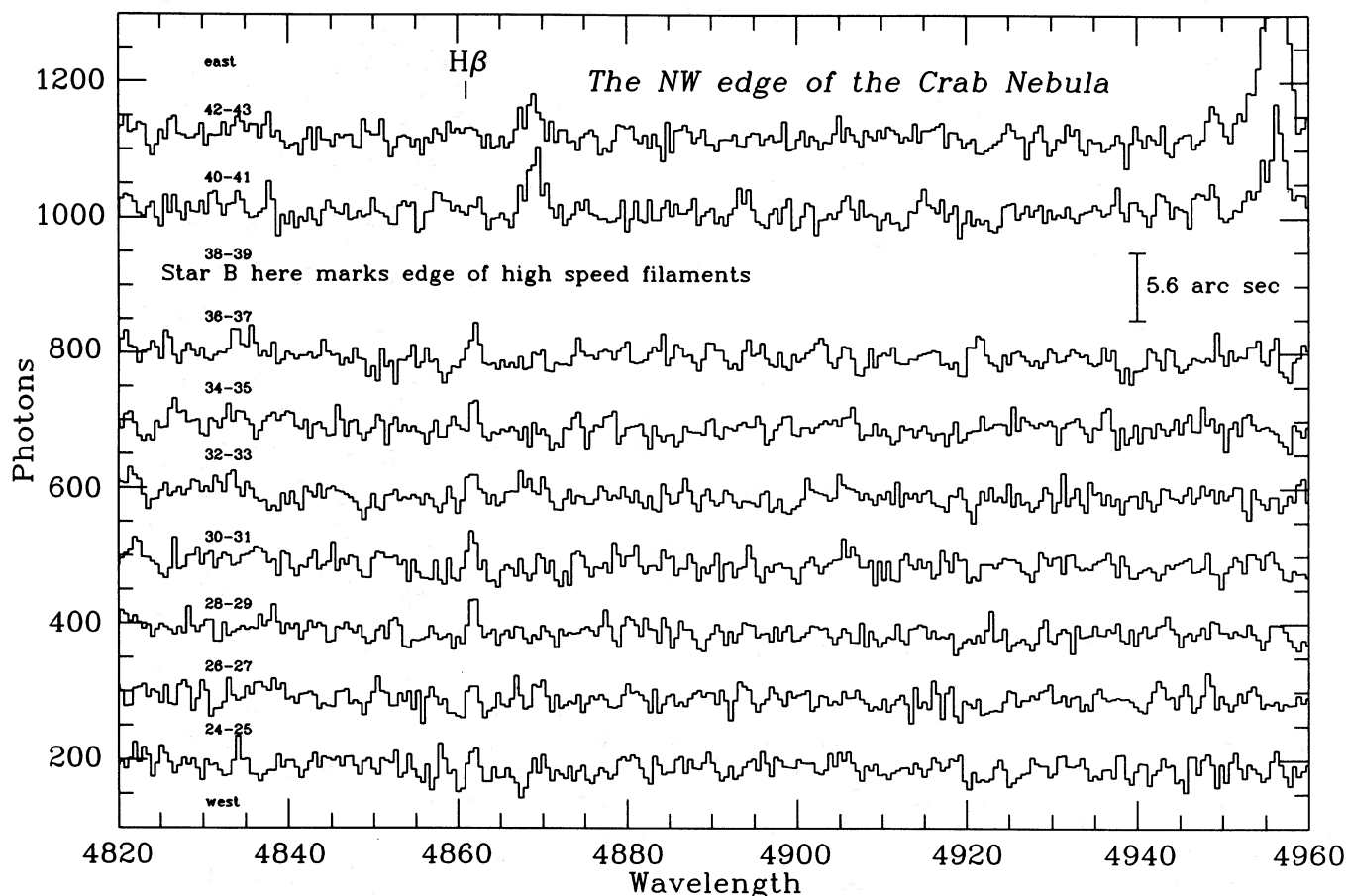


Figure 4. Spatially resolved spectra of the edge of the Crab nebula. As Fig. 3, but plotted at twice the spatial resolution (and correspondingly half the recorded flux), in order to show the abrupt change in the narrow-line $H\beta$ emission at the filaments.

consequence of the clumpiness of the halo and the fact that the data are drawn from different quadrants, as well as observational error).

The density of the halo, where detected, is of order 1 cm^{-3} , if the temperature is 7000 K. The lack of $[O\text{III}]$ could indicate a high ionization, at high temperature and a lower density (Lundqvist et al. 1986). A value of 1 cm^{-3} is considerably in excess of the density deduced by Bietenholz et al. (1991) from the lack of deceleration of the Crab's expansion. An alternative explanation may be non-spherical symmetry. A spectrum that is more informative than one just showing $H\beta$ would help determine the temperature. Until the halo is well mapped three-dimensionally, and its temperature determined, the mass estimate of the halo must be regarded as preliminary.

5 CONCLUSION

The mass of the Crab progenitor was thus some 4 to $6 M_{\odot}$ in addition to the pulsar and filaments, namely in excess of $7 M_{\odot}$, consistent with the $8 M_{\odot}$ lower limit to the mass of Type II supernovae and the abundance of elements in the filaments. A significant fraction – half – of the mass of the

progenitor had been lost by its stellar wind, and the mass of the envelope and mantle packed around the core at the time of explosion was thus much reduced. The similarity in this respect between SN 1054, SN 1987A and SN 1993J is apparent.

ACKNOWLEDGMENTS

I especially pay tribute to Roger Chevalier's inspired persistence in the belief that the Crab nebula must show a halo, however faint and difficult to observe, and for his encouragement to carry out this work. Rob Fesen provided a characteristically open, vigorous, helpful and sceptical referee's report. I thank Robin Clegg, Robert Cumming, Peter Meikle and Janet Sinclair of the RGO for assistance in reducing the data and preparing this paper, and also for their comments. I am extremely grateful to Robin Catchpole for finding the Schmidt plate. I also thank Harvey MacGillivray, of ROE's Wide Field Astronomy facilities, who so promptly scanned the UK Schmidt Telescope plate for me and made Fig. 1. The Isaac Newton Telescope on the island of La Palma is operated by the Royal Greenwich Observatory at the Spanish Observatorio del Roque de los Muchachos of the Instituto de Astrofísica de Canarias.

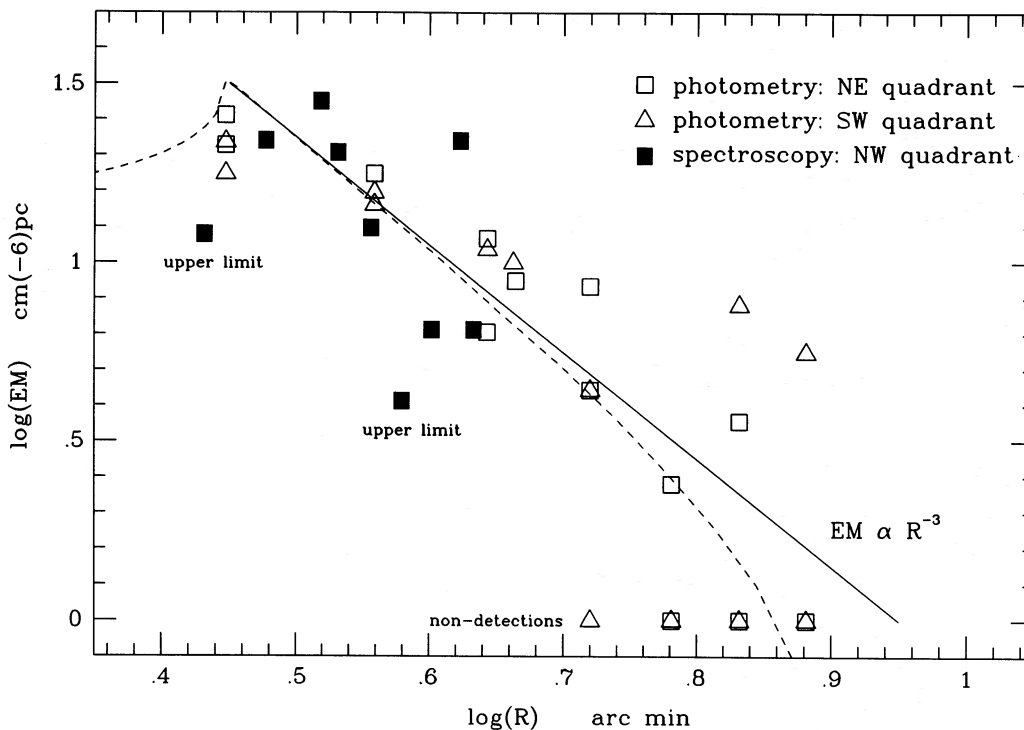


Figure 5. Spatial distribution of surface brightness of the Crab nebula halo. EM is emission measure, and different symbols denote the present spectroscopic results (filled squares) and previous photometric results (open symbols, data taken from fig. 1 of Murdin & Clark 1981). The innermost spectroscopic point is an upper limit for the detection of zero-velocity $H\beta$ amongst the confusion of the high-speed filamentary emission. Points plotted at $\log(EM) = 0$ are non-detections, or negative detections (statistical fluctuations below background). The scatter of the points is a result of observational error, the clumpiness of the halo and the combination of data from different quadrants. The solid line represents an extensive, spherically symmetric, outflowing stellar wind of constant speed; the line has slope of -3 , and the model is fitted to the data by eye. The dashed line is a fit for the same stellar wind model bounded by an inner and an outer sphere at radii of 2.8 and 8 arcmin, respectively. The observed high contrast and abrupt drop in emission measure at the inner boundary are poorly reproduced by the hollow model.

REFERENCES

- Bietenholz M. F., Kronberg P. P., Hogg D. E., Wilson A. S., 1991, *ApJ*, 373, L62
- Chevalier R., 1977, in Schramm D. N., ed., *Supernovae*. Reidel, Dordrecht, p. 53
- Chevalier R., 1985, in Kafatos M. C., Henry R. C., eds, *The Crab Nebula and Related Supernova Remnants*. Cambridge Univ. Press, Cambridge, p. 63
- Chevalier R., 1994, in Proc. IAU Colloq. 145, *Supernovae and Supernova Remnants*. Xian China, in press
- Clark D. H., Murdin P., Wood R., Gilmozzi R., Danziger I. J., Furr A. W., 1983, *MNRAS*, 204, 415
- Davidson K., 1985, in Kafatos M. C., Henry R. C., eds, *The Crab Nebula and Related Supernova Remnants*. Cambridge Univ. Press, Cambridge, p. 73
- Davidson K., Fesen R. A., 1985, *ARA&A*, 23, 119
- Dennefeld M., Pequignot D., 1983, *A&A*, 127, 42
- Fesen R. A., Blair W. P., 1990, *ApJ*, 351, L45
- Fesen R. A., Ketelsen D. A., 1985, in Kafatos M. C., Henry R. C., eds, *The Crab Nebula and Related Supernova Remnants*. Cambridge Univ. Press, Cambridge, p. 89
- Gull T. R., Fesen R. A., 1982, *ApJ*, 260, L75
- Henry R. B. C., MacAlpine G. M., 1982, *ApJ*, 258, 11
- Lundqvist P., Fransson C., Chevalier R., 1986, *A&A*, 162, L6
- MacAlpine G. M., Uomoto A., 1991, *AJ*, 102, 218
- MacAlpine G. M., McGaugh S. S., Mazzarella J. M., Umoto A., 1989, *ApJ*, 342, 364
- Mathis J. S., 1986, *ApJ*, 301, 423
- Matveenko L. I., 1984, *SvA Lett.*, 10, 44
- Miller J. S., 1973, *ApJ*, 180, L83
- Murdin P., Clark D. H., 1981, *Nat*, 294, 543
- Murdin P., Murdin L., 1984, *Supernovae*. Cambridge Univ. Press, Cambridge, p. 112
- Nomoto K., 1985, in Kafatos M. C., Henry R. C., eds, *The Crab Nebula and Related Supernova Remnants*. Cambridge Univ. Press, Cambridge, p. 97
- O'Dell C. R., 1962, *ApJ*, 136, 809
- Osterbrock D. E., 1989, *Astrophysics of Gaseous Nebulae and Active Galactic Nuclei*. University Science Books, Mill Valley, California
- Reynolds R. J., 1987, *ApJ*, 323, 118
- Trimble V., 1970, in Davies R. D., Smith F. G., eds, *Proc. IAU Symp. 46, The Crab Nebula*. Reidel, Dordrecht
- Trimble V., 1973, *PASP*, 85, 579
- Trimble V., 1977, *Astrophys. Lett.*, 18, 145
- van den Bergh S., 1994, in Proc. IAU Colloq. 145, *Supernovae and Supernova Remnants*. Xian China, in press
- Van Dyk S. D., Sramek R. A., Weiler K. W., Panagia N., 1993, *ApJ*, 409, 162
- Velusamy T., 1984, *Nat*, 308, 251
- Wilson A. S., Weiler K. W., 1982, *Nat*, 300, 155
- Woltjer L., 1957, *Bull. Astron. Inst. Neth.*, 13, 301